Dahal, Roshi; Uusi-Kyyny, Petri; Pokki, Juha-Pekka; Ohra-aho, Taina; Alopaeus, Ville

Conceptual design of a distillation process for the separation of styrene monomer from polystyrene pyrolysis oil: experiment and simulation

Published in:
Chemical Engineering Research and Design

DOI:
10.1016/j.cherd.2023.05.039

Published: 01/07/2023

Document Version
Publisher's PDF, also known as Version of record

Available online at www.sciencedirect.com

Chemical Engineering Research and Design

journal homepage: www.elsevier.com/locate/cherd

Conceptual design of a distillation process for the separation of styrene monomer from polystyrene pyrolysis oil: experiment and simulation

Roshi Dahal[a,*], Petri Uusi-Kyyny[a], Juha-Pekka Pokki[a], Taina Ohra-aho[b], Ville Alopaeus[a]

[a] Aalto University, School of Chemical Engineering, Department of Chemical and Metallurgical Engineering, P.O. Box 11000, FI-00076 Aalto, Finland

[b] VTT – Technical Research Centre of Finland, Tietotie 4C Espoo, Finland

ARTICLE INFO

Article history:
Received 30 November 2022
Received in revised form 15 February 2023
Accepted 15 May 2023
Available online 19 May 2023

Keywords:
Plastic waste
Pyrolysis
Batch distillation
Short-path distillation
Styrene monomer

ABSTRACT

This study presents experiments and modeling of batch distillation for the separation of styrene monomer from polystyrene pyrolysis oil. The bottoms obtained from the batch distillation was further fractionated applying a short-path distillation unit to study the separation efficiency of styrene from the polystyrene pyrolysis oil. GC-FID and GCMS were applied for the composition analysis of the polystyrene pyrolysis oil, distillate, and bottom fractions. Styrene monomer was obtained with a purity of 99.9 wt% from the batch distillation. The batch distillation was modeled employing the NRTL–RK thermodynamic model. A good agreement was achieved for the purity of styrene between the experimental analysis and model prediction. Additionally, a continuous distillation column was modeled for the scale-up of the process. Furthermore, viscosities and densities of the bottoms fraction were measured at the temperature range of 298–348 K.

1. Introduction

The low recycling rates and increasing production of plastics have resulted in accumulation of discarded plastics in landfills (Barnes et al., 2009) and oceans (Jambeck et al., 2015), and requires development of new and efficient technologies for waste recycling (Qureshi et al., 2020; Rahimi and Garciá, 2017). On the other hand, global warming and the current energy shortage have directed research efforts to finding alternative and sustainable energy sources. Traditionally produced from petroleum by-products, plastic polymers are rich in hydrocarbons (Hopewell et al., 2009). Moreover, valorization of plastic waste to produce chemicals and fuel can fulfill energy demand and provide economic and environmental benefits.

Even though plastics recycling symbol was initiated 40 years ago, only 14% of plastic packaging is collected for recycling globally, and the recycling rate for plastics is much lower than for plastics packaging (Ellen MacArthur Foundation, 2017). In Europe, 10% of plastic waste is recycled by applying mechanical recycling routes (Qureshi et al., 2020). Therefore, the chemical recycling of waste plastics via pyrolysis is gaining interest these days due to the need for recycling of the high share of plastics which cannot be mechanically recycled. Chemical recycling technologies (Grause et al., 2011) can possibly play an important role in the transition towards a circular economy (Qureshi et al., 2020). The closed loop recycling of materials (Qureshi et al., 2020) as well as hydrocarbons with excellent fuel properties (Sharma et al.,

Abbreviations: PS, polystyrene

* Corresponding author.
E-mail address: roshi.dahal@aalto.fi (R. Dahal).

https://doi.org/10.1016/j.cherd.2023.05.039

Nomenclature

Abbreviations

αMS	alpha-Methylstyrene
CAS	Chemical Abstracts Service Registry Number
exp	experimental
FID	Flame Ionization Detector
GC	Gas Chromatography
HETP	Height Equivalent Theoretical Plate
lit	literature
MS	Mass Spectroscopy
ppm	parts per million
rpm	rotations per minute
VLE	Vapor–Liquid Equilibrium
wt	weight

Symbols

F	flowrate
g	gram
mbar	millibar
mL	milliliter
mm	millimeter
P	pressure (mbar)
T	temperature (K)
W	Watt

2014) can be achieved. In addition, if pure monomer could be recovered through chemical recycling, the price of polymers could be decoupled from the oil prices (Rahimi and Garciá, 2017).

Liu and co-authors (Liu et al., 2000) have studied pyrolysis of polystyrene waste in a fluidized bed reactor to obtain styrene monomer and gasoline fraction. The yield of styrene from the pyrolysis was 78.7 wt%. Styrene monomer was obtained with a purity of 99.6 wt% from the vacuum distillation of pyrolysis oil. In addition, Liu and co-authors have discussed about the recycling of the bottoms fraction to the pyrolysis reactor to increase the yield of styrene and aromatics in the pyrolysis oil.

Within these contexts, this study presents the purification of polystyrene pyrolysis oil to polymerization grade styrene by employing distillation to obtain styrene monomer which could be re-polymerized in the production of latex or other polymers. Styrene monomer was obtained with the purity of 99.9 wt% from the batch distillation of polystyrene (PS) pyrolysis oil. The predicted purity of styrene from the batch distillation model was comparable with the experimental analysis. Additionally, a continuous distillation was modeled for scale-up of the process. The binary interaction parameters for styrene + toluene/α-methylstyrene were adopted from the previous VLE work (Dahal et al., 2023) and applied to improve the distillation model. In addition, the physical properties of the bottoms fraction were measured which can be employed for the design of the pumps.

This work outlines the separation of styrene monomer from polystyrene pyrolysis oil where polymerization grade styrene was achieved with higher purity (99.9 wt%) than in the literature (99.6 wt%) (Liu et al., 2000). Additionally, this research is a comprehensive study for the fractionation of polystyrene pyrolysis oil which includes phase equilibria and distillation combined with the physical properties of the bottoms fraction.

2. Experimental

This section details about the experimental procedure applied for the purification of polystyrene pyrolysis oil.

2.1. Pyrolysis

This research was initiated by applying pure polystyrene (PS) as a feedstock for pyrolysis to obtain a better understanding of the system at the beginning. The model feedstock was processed with a modular extruder for homogenization and densification. The homogenized polystyrene feedstock was pyrolyzed under various conditions: (1–8) second/s of residence time and a 450–550 °C range of temperature. The PS pyrolysis oil was obtained with a styrene content of 71.5 wt% at a pyrolysis temperature of 550 °C. The pyrolysis was performed at VTT Technical Research Center of Finland Ltd.

2.2. Materials

PS pyrolysis oil was characterized by employing Gas Chromatograph Mass Spectrometer (GCMS). Thereafter, the retention time of PS pyrolysis oil components in Gas Chromatograph (GC) equipped with Flame Ionization Detector (FID) were determined by applying the pure components provided in Table 1. 2,4-trimethyl-1-pentene and 2,2,4-trimethyl-2-pentene were employed for the distillation column characterization. 4-tert-Butylcatechol was adopted as a polymerization inhibitor during distillation of the PS pyrolysis oil. 1,2-Diphenylethane (bibenzyl) was applied as the styrene dimer model component.

2.3. Fractionation

The separation of pure styrene monomer from the PS pyrolysis oil was studied at Aalto University by applying batch distillation. The styrene content in the bottoms fraction after batch distillation was 39.5 wt% as presented in Table 2. Therefore, the bottoms fraction from the batch distillation of PS pyrolysis oil was further fractionated by applying a short-path distillation (SPD) unit. The objective of the SPD was to study the separation of most of the styrene from the PS pyrolysis oil.

2.3.1. Batch distillation column

The batch distillation column consists of a two-section setup with the structured packing (MONTZ type A3–1000) internals specification given as 1000 m^2/m^3 specific surface, 80 mm height and 25.2 mm diameter. The upper and the lower sections of the column included 14 and 7 pieces of packing, respectively. Both the upper and lower sections were comprised of a DN25 diameter silver coated column (NORMAG GmbH, Ilmenau, Germany) with vacuum isolation, sight stripes, and outer expansion bellows. The total heights of the upper and the lower sections of the column were 1330 mm with a packing height of 1120 mm and 690 mm with a packing height of 560 mm, respectively. The heating mantle (ITA Instruments) was applied for the reboiler. A round

Table 1 – List of the materials and their specifications.

Component/CAS number	Supplier/Purity
PS pyrolysis oil components	
Acetone/67–64–1	VWR Chemicals/ > 99.9%
Benzene/71–43–2	Sigma-Aldrich/ > 99.9%
Ethylbenzene/100–41–4	Sigma-Aldrich/ > 99.0%
α-Methylstyrene/98–83–9	Sigma-Aldrich/ 99%, 15 ppm* *p-tert*-butylcatechol[a]
Phenylacetylene/536–74–3	Sigma-Aldrich/ 98.0%
2-Propenyl benzene/300–57–2	Sigma-Aldrich/ > 98.0%
Styrene/100–42–5	Sigma-Aldrich/ ≥ 99.9%, 10–15 ppm* 4-*tert*-butylcatechol[a]
Toluene/108–88–3	VWR Chemicals/ ≥ 99.95%
o-Xylene/95–47–6	Sigma-Aldrich/ > 99.0%
p-Xylene/106–42–3	Sigma-Aldrich/ > 99.0%
m-Xylene/108–38–3	Sigma-Aldrich/ > 99.0%
Dimer model component	
1,2-Diphenylethane/103–29–7	Sigma-Aldrich/ 99%
Components for distillation column characterization	
2,2,4-trimethyl-1-pentene/107–39–1	Sigma-Aldrich/ 99%
2,2,4-trimethyl-2-pentene/107–40–4	Sigma-Aldrich/ 99%
Polymerization inhibitor	
4-*tert*-butylcatechol/98–29–3	Sigma-Aldrich/ ≥ 99%

* Parts per million.
[a] Inhibitor content according to supplier.

bottom reboiler flask was kept inside a polycarbonate box provided with nitrogen purging for safety. The distillation column was placed inside a six-meter-high polycarbonate cabin equipped with ventilation.

The Pt-100 temperature probes were applied to measure temperatures of the reboiler, the condenser and the middle section of the column. The pressure transducer was located at the top of the condenser. The thermometer probes and the pressure transducer were wired to National Instruments cRIO-9045 connected to a computer with National Instruments LabVIEW software. The masses were measured with an electronic balance (OHAUS AX8201) and the uncertainty of the measured mass was 0.1 g. The uncertainty in measured temperatures were 0.2 K for the bottom and 0.3 K for the distillate, and 0.1 kPa for the pressure measurement.

2.3.2. *Short-path distillation unit*

The bottoms obtained from the batch distillation was further fractionated by applying a KDL1 laboratory-scale short-path distillation unit (UIC GmbH, Alzenau-Hoerstein, Germany).

Table 2 – Gas chromatography analysis of the PS pyrolysis oil, distillates and the bottoms obtained from the experimental batch distillation.

components	composition (mass fraction)						
	PS pyrolysis oil	distillate fractions					bottoms
		1st	2nd	3rd	4th	5th	
Lighter							
Acetone	1.43E-05	1.80E-04	0	0	0	0	0
Benzene	3.97E-06	5.00E-05	0	0	0	0	0
Toluene	5.93E-03	7.39E-02	2.25E-04	2.3E-04	0	0	0
Ethylbenzene	1.51E-03	1.10E-02	3.05E-03	1.66E-03	7.8E-04	2.7E-04	0
p-Xylene	5.87E-05	1.70E-04	0	1.0E-04	2.1E-04	2.0E-05	0
o-Xylene	4.10E-05	2.40E-04	3.0E-05	7.0E-05	5.0E-04	3.0E-05	0
m-Xylene	1.17E-04	4.20E-04	6.0E-05	2.30E-04	2.9E-04	5.0E-04	0
2-propenylbenzene	1.59E-06	2.00E-05	0	0	0	0	0
Phenylacetylene	3.89E-05	1.10E-04	8.0E-05	7.0E-05	7.0E-05	6.0E-05	0
Cumene	1.02E-05	0	0	3.0E-05	3.0E-05	3.0E-05	0
Styrene	**0.7159**	**0.9137**	**0.9941**	**0.9974**	**0.9985**	**0.9994**	**0.3951**
Heavies							
α-Methyl styrene	1.06E-02	0	0	0	0	0	2.31E-02
β-Methyl styrene	9.07E-04	0	0	0	0	0	1.24E-03
3 butenyl benzene	8.03E-04	0	0	0	0	0	1.41E-03
1 H-Indene	3.38E-03	0	0	0	0	0	7.38E-03
Divinylbenzene isomers	2.05E-03	0	0	0	0	0	2.04E-03
Dimers	0.1811	0	0	0	0	0	0.3965
Heavier fraction	0.0776	0	0	0	0	0	0.1694

$u(w_{distillate}) = 0.00004$, $u(w_{bottoms}) = 0.004$.

The operating principle of the short-path distillation unit adopted in this work is as similar as presented by Kim and co-authors (Kim et al., 2021). The evaporator was made up of borosilicate glass with an evaporation surface area of 0.017 m^2 and equipped with motor-driven roller wiper to create a thin film of liquid on the inner wall by centrifugal force. The temperatures of the feed tank and the evaporator were maintained by a jacket circulated with hot oil (FG heat transfer fluid, Petro-Canada Lubricants). A vacuum system was connected to maintain the operating pressure within the system. The pressure of the system was adjusted using a pressure-regulating valve for air. The pressure readings were taken using a vacuum gauge (DCP 3000 Vacuubrand). The water-cooled condenser allowed the vapor to condense as distillate, and non-volatiles were collected as bottoms residue. A liquid nitrogen trap served as a protection for the vacuum system by condensing the vapor leaving the condenser.

2.4. Batch distillation column characterization

The experimental work began with a determination of the number of theoretical stages, the height equivalent of theoretical plates, the pressure drop, the heat losses of the column and the column hold-up.

2.4.1. Number of theoretical stages

A gravimetric mixture of 2,2,4-trimethyl-1-pentene (TM1P) and 2,2,4-trimethyl-2-pentene (TM2P) was distilled under atmospheric pressure and total reflux conditions until a steady state temperature profile was established in the column. Thereafter, the samples from distillate and bottoms were taken and analyzed by GC. Then, the number of theoretical stages (24 ± 1 stages) was graphically determined by applying the McCabe-Thiele method (Seader et al., 2008). Next, the height equivalent theoretical plate (HETP) was calculated by employing the number of theoretical stages (24) and the total packing height (1680 mm), which is equal to 69 ± 2 mm.

2.4.2. Pressure drop

The pressure drop of the column was determined by heating a mixture of TM1P and TM2P at atmospheric pressure. The pressures were measured by the pressure sensors located at the bottom (reboiler), the middle section, and the top of the column. The calculated pressure drop from the top to the bottom of the column was 0.9 ± 0.1 mbar.

This pressure drop is not precisely transferable to other experiments because the density of the vapor phase at the atmospheric pressure is appr. 10 times larger than in the vacuum. However, the F-factor for the TM1P + TM2P mixture and the polystyrene pyrolysis oil mixture was compared. Firstly, the F-factor was calculated applying Eq. (1). Secondly, the calculated F-factors were applied in the pressure drop correlation for the Montz packing A3–1000 to obtain the pressure drop. The pressure drop for the pyrolysis oil distillations was 0.6 mbar/m at the top part of the column and 1 mbar/m at the lower part of the column. This shows that the pressure drop is comparable to the representative pressure drop measurement of the TM1P + TM2P mixture.

$$F\ \ factor = w_G{}^{*}\sqrt{\rho_G} \tag{1}$$

where w_G is the superficial velocity (m/s) and ρ_G is the gas density (kg/m^3).

2.4.3. Heat losses

The heat loss in the column was also determined using the mixture of TM1P and TM2P. Two separate experiments were conducted by applying a) a reboiler flask insulated with fiberglass cloth and b) a reboiler flask without insulation. The power of the reboiler was adjusted to 320 W for the reboiler flask without insulation and to 400 W for the insulated reboiler flask. The mixture was heated under total reflux until a constant temperature profile (100 °C) was observed. Then, the mass of the distillate under zero reflux within the time interval of 15, 30, 45 and 60 s was measured. Thereafter, the power required to vaporize the distillate was calculated applying Eq. (2).

$$P = \frac{n}{\Delta t}\ \ \Delta H_{vap} \tag{2}$$

where P is power (J/s), n is moles of distillate (mol), t is time (s), and ΔH_{vap} is heat of vaporization (J/mol) of TM1P. The calculated power was compared to the power output of the reboiler and the heat losses were calculated as: 61 ± 5% of reboiler output for the insulated reboiler and 80 ± 1% of reboiler output for the reboiler without insulation.

The approximate enthalpy change of the mixture from liquid to vapor can be calculated using the mole fraction and the pure component enthalpy of vaporization. In this experiment, the mole fraction of TM1P was 0.506 in the reboiler and 0.914 in the distillate. If the pure TM1P enthalpy of vaporization at 100 °C is compared with the approximate enthalpy change, the percent difference in the reboiler and the distillate is 2% and 0.4% respectively. This minor difference is assumed to have a minimal effect in the distillation column characterization. Therefore, only the heat of vaporization of TM1P was applied in Eq. (2) to calculate the power required to vaporize the distillate.

From the calculation, it can be observed that the heat losses are large. However, the total height of the column is approximately 4 m, and the surface area of the column, the spherical glass joints and the conical glass joints are large. The transmission of this calculated heat loss to pyrolysis oil distillation is reasonable because the distillation of polystyrene pyrolysis oil was started at a temperature below 100 °C and approached 110 °C at the end. The average heat loss along the time scale of the polystyrene pyrolysis oil distillation is comparable to the steady temperature of the TM1P + TM2P mixture.

2.4.4. Column hold-up

The batch distillation column hold-up experiment was performed (at 95 mbar) by employing two components with a substantial difference in boiling points: toluene and ethylbenzene. During the experiment, ethylbenzene was loaded into the flask and boiled under total reflux until a constant temperature profile was formed in the column. Then, toluene was added in small amounts through a capillary placed next to the reflux rate controller at the top of the column. Toluene was added until the whole top section of the column (14 packings) was wetted with it. This was observed when the thermometer reading between the two sections reached the

boiling point of pure toluene. The mass of the toluene added to the top section (14 packings) of the column was 46.1 g. Thus, the column hold-up calculated was 3.3 ± 0.2 g for 80-mm length piece of packing.

Furthermore, the liquid hold-up of a single packing (Montz Type A3–1000) was determined employing toluene. Initially, a single packing was weighed (dry mass), and the packing was completely submerged into pure toluene. The submerged packing was lifted with a tweezer and placed in an empty decanter glass. The mass of the packing was weighed (wet mass). The procedure was followed quickly because toluene could evaporate rapidly during the measurements. Four experimental repetition was performed at the room temperature and the ambient pressure. Afterwards, the single packing hold-up was determined from the dry and wet masses of the single packing. The calculated single packing hold-up was 3.5 ± 0.2 g/packing. It can be noticed that the single packing hold-up (3.5 g/packing) is slightly higher than the batch distillation column hold-up (3.3 g/packing). However, the single packing hold-up was determined at ambient conditions whereas the batch distillation column hold-up measurement was carried out at different temperature-pressure conditions (95 mbar). The difference in the viscosities of toluene at these two different conditions could possibly result in such a difference.

Next, the viscosity and the surface tension of toluene, ethylbenzene and styrene was calculated applying the DIPPR correlation (Design Institute for Physical Properties, 2005) and plotted as a function of temperature 25–125 °C. The relative deviations of the viscosity of styrene from the viscosity of toluene and ethylbenzene were 10% and 3%, respectively. Similarly, the relative deviations of the surface tension of styrene from the surface tension of toluene and ethylbenzene were 13% and 8%, respectively. These differences were assumed to have a minor effect on the column characterization. Hence, the column hold-up measurements employing toluene and ethylbenzene is relatable for other components of the polystyrene pyrolysis oil.

2.5. Experimental distillation runs

This section details the experimental conditions applied during the batch and the short-path distillations.

2.5.1. Batch distillation

The PS pyrolysis oil distillation was carried out in the batch mode under vacuum at 99 ± 2 mbar of the condenser pressure. The reboiler flask was insulated with a fiberglass cloth and the reboiler was operated at the power of 160 W. 4-*tert*-Butylcatechol was added to the PS pyrolysis oil batch prior to the distillation and to each distillate collector in the concentration of 10 ppm to inhibit the polymerization of styrene. Five distillate fractions were taken. The reflux ratio was set to three for the first distillate fraction and then to one for the other four fractions.

About 60 mL of the distillate was planned to obtain at an interval of 30–45 min from the batch distillation experiments. The low boiling components were separated from the first two distillate fractions. Thereafter, it was possible to get pure styrene monomer in the later distillate fractions. After the collection of distillates in the distillate collector flask, the distillate collector flask was detached from the batch distillation column. The distillate was poured into a glass bottle and the mass of the distillate was weighed. Thereafter, the distillate collector flask was connected back to the distillation column. All five distillate fractions were collected applying the same procedure. However, the batch distillation run was stopped at a bottom temperature of 100–120 °C to minimize the risk of polymerization.

2.5.2. Short-path distillation

The short-path distillation (SPD) was initiated with a test distillation using toluene to estimate the heat transfer capacity. The operational conditions ($T = 70$ °C, $P = 270$ mbar) were specified using the vapor pressure curve of toluene from the DIPPR correlation (Design Institute for Physical Properties, 2005). Based on the test distillation, the calculated heat transfer capacity of the SPD unit was 0.38 W/K. It was assumed that the heat transfer for the actual sample distillation is the same as in the test distillation.

The distillation of the bottoms obtained from the batch distillation was carried out at 80 mbar, and 110 °C of evaporation temperature. The rotational speed of roller wiper was set to 106 rpm and the condensation temperature was 26 °C. The feed flow was kept at 0.31 mL/min. Prior to the short-path distillation, 4-tert-butylcatechol was added to the bottoms (0.002 g) and the distillate collection flasks (0.001 g) to avoid polymerization.

2.6. Characterization

The characterization techniques employed for the distillate and the bottom fractions is presented in the following sections.

2.6.1. GC analysis

All the distillate and the bottoms fraction obtained from the batch distillation and the SPD were taken into vials and analyzed directly after the completion of experiments. The toluene present in the PS pyrolysis oil was separated from the distillates and no remains were left in the bottom fraction (Table 2). Therefore, toluene was applied as an internal standard (solvent) for the analysis of bottoms fraction. The heavy components that cannot be detected from the GC was quantified applying the mass of internal standard. However, the distillate fractions were analyzed without an addition of solvent because the distillate fractions mainly consist of pure styrene.

Agilent 6850 GC equipped with FID was employed for the quantitative analysis of the distilled fractions. The analysis of the components is based on the method of peak area, and priorly determined retention times for the pure components. GC settings applied for the analysis of the bottoms (method I) and the distillates (method II) is illustrated in Appendix Table A-1. Further, Shimadzu GCMS–QP2010 SE was employed for the identification of the components in the distillate and the bottoms fractions. The runs in the GCMS instrument were made by applying the same capillary column and GC settings (Appendix Table A-1) as adopted for the Agilent 6850 GC. The identified peaks were compared with the MS of the components provided in the Pyrolysis–GC/MS data book (Tsuge et al., 2011) as well.

2.6.2. Density & viscosity

A DMA 5000 M density meter (Anton Paar GmbH, Graz, Austria) was adopted for the density measurements of the bottoms fraction. The temperature uncertainty of the density meter provided by the manufacturer was 0.1 K. The expanded uncertainty of the density measurement was estimated to be 0.3 kg m^{-3} at the 95% level (Baird et al., 2017). Further, a Brookfield LVDVE230 rotational viscometer was applied to measure viscosities of the bottoms fraction. The temperature was controlled employing a Lauda water bath (u (T) = 0.2 K). The temperature was let to stabilize for 30 min before recoding the viscosity value at every temperature change. The uncertainty includes the standard uncertainty of the viscometer (10%) and the uncertainty in measurement repeatability. Then, the expanded uncertainty was calculated employing the method as described in earlier work (Dahal et al., 2021).

2.7. Laboratory saftey

The polystyrene pyrolysis oil components are hazardous, and some are carcinogenic, therefore; precautions were applied during the experimental work to avoid human damage or any kind of contamination in the laboratory premises. The distillation apparatus was placed inside a polycarbonate cabinet with a ventilation system and a nitrogen purging to the reboiler cabinet. The powered air-purifying respirator was adopted while handling the pyrolysis oil and performing distillations. In addition to these, the safety guidelines provided in the safety data sheet for handling styrene and its waste was followed.

3. Batch distillation modeling

The batch distillation was modeled using the Non–Random Two–Liquid (NRTL) (Renon and Prausnitz, 1968) activity coefficient model and Redlich–Kwong (RK) equation of state for the vapor phase fugacity (Redlich and Kwong, 1949) in Aspen Plus version 11. The vapor phase fugacity coefficients and the Poynting correction were included in the model even though both the values were very close to one in this case. The pure component properties were retrieved with the Aspen Plus from the NIST Thermo Data Engine database version 10.2. The PS pyrolysis oil composition provided in Table 2 was applied as a feed in the simulation. Further, the heavier components were lumped as heavy and designated as styrene trimer which is non-volatile. The binary parameters for every component pair in Table 2 were taken from the Aspen Plus Databank (APV110 VLE–RK). In addition, the binary interaction parameters for styrene + αMS and toluene + styrene were adopted from the previous work (Dahal et al., 2023). The batch distillation column was assumed to consist of 24 theoretical stages based on the earlier column analysis (Section 2.4.1). The experimentally determined operational specifications such as the holdup, the reboiler duty, the heat loss, the pressure, the reflux ratio, the operating steps, and the masses of the feed and the distillates were employed in the batch model. The heat loss was specified as a side duty.

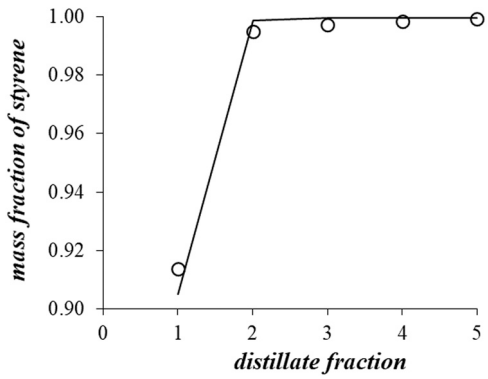

Fig. 1 – Purity of styrene in five distillate fractions: (o) exp and (—) from the batch model.

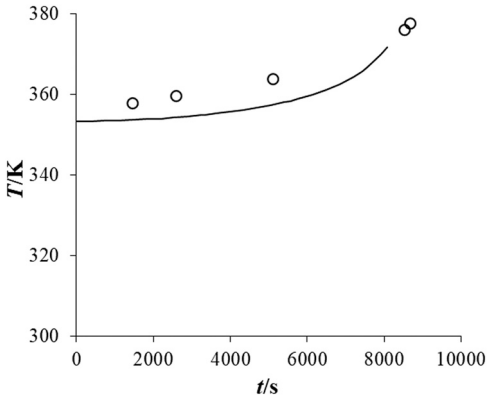

Fig. 2 – Reboiler temperature and the batch distillation time profile: (o) exp distillate fraction and (—) from the batch model.

4. Results

This section summarizes the results from the experimental batch distillation and the batch distillation model. The results from the GC analysis and the short-path distillation are detailed. The measured physical properties of the bottom fraction are provided in the Supporting Information.

4.1. Batch distillation

Table 2 presents the GC analysis of the PS pyrolysis oil, the distillates and the bottoms obtained from the batch distillation. The low boiling fractions such as acetone and benzene were present only in the first distillate fraction. Styrene was obtained with the purity of 0.9994 in mass fraction in the fifth distillate fraction. Further, the bottoms fraction consists of styrene and heavies only. The experimentally determined purity of styrene in five distillate fractions agree well with the calculated one from the batch model in Fig. 1. The mass fraction of styrene in the bottoms from the experimental analysis and predicted from the model were 0.395 and 0.442, respectively. Furthermore, the experimental temperature and the time profiles are comparable with the calculated ones in Fig. 2.

Table 3 – The masses (g) of the feed, distillates, bottoms and the loss amount measured in the experimental batch distillation of PS pyrolysis oil.

feed	distillates					bottoms	loss
	1st	2nd	3rd	4th	5th		
552.2	43.8	46.6	89.9	73.6	24.8	252.4	21.1

The uncertainty of measured mass is 0.1 g.

Table 4 – Gas chromatograph analysis of the distillate and the bottom fractions of the short-path distillation.

components	composition (mass fraction)	
	distillate	bottoms
Styrene	**0.7775**	**0.0631**
Heavies		
α-Methyl styrene	0.0472	0.0031
β-Methyl styrene	0.0025	–
3 butenyl benzene	0.0029	0.0002
1 H-Indene	0.0148	0.0014
Divinylbenzene isomers	0.0054	0.0004
Dimers	0.1443	0.5725
Heavier fractions	–	0.3597

$u(w_{distillate}) = 0.004$, $u(w_{bottoms}) = 0.004$.

Table 3 presents the measured masses of the feed, the distillates, and the bottoms during the experimental batch distillation. In Table 3, the loss amount is a residual hold-up of the batch distillation column. This residual hold-up is equal to 30% of the total column hold-up (in Section 2.4.4) during the operation.

4.2. *Short-path distillation*

The feed for the short-path distillation is the bottoms obtained from the batch distillation and the composition is presented in Table 2. Table 4 presents the GC analysis of the distillate and the bottoms obtained from the short-path distillation. The masses of the feed, the distillate and the bottoms measured in the short-path distillation are presented in Table 5. The loss amount in Table 5 is a residue in the short-path distillation unit which was not recovered.

As there is no reflux in the short-path distillation, it is difficult to obtain a pure styrene monomer with this method. However, the motive of the short-path distillation was to investigate the separation of residual styrene from the heavier but potentially close-boiling pyrolysis oil fractions. The short residence time and the low pressures were required for the polystyrene pyrolysis oil distillation due to potential side reactions, and the system can undergo polymerization. These conditions were achievable in the SPD unit.

The concentration of styrene in the bottoms after the short-path distillation was only 6 wt% as presented in Table 4. Apart from the lighter components, α-methylstyrene (αMS) seems a possible component from the heavier end to affect the purity of styrene during the separation which is observed from Table 4. Therefore, the VLE of styrene + αMS

Table 5 – The masses (g) of the feed, distillate, bottoms and the loss amount measured in the experimental short-path distillation.

feed	distillate	bottoms	loss
35	13.4	19.9	1.7

The uncertainty of measured mass is 0.1 g.

was measured in our previous work (Dahal et al., 2023) and the parameters were adopted for the distillation column modeling in this work as mentioned in the Section 1.

Overall, the batch distillation and the short-path distillation of the PS pyrolysis oil exhibits that the separation of most of the styrene from the PS pyrolysis oil is achievable. The overall loss of the styrene from the initial PS pyrolysis oil was only 0.3 wt%. Thus, the distillation seems an efficient separation method for the purification of PS pyrolysis oil.

5. Continuous distillation column modeling

This section proposes a process scheme and discusses the model predictions for the separation of styrene monomer from the PS pyrolysis oil.

5.1. *Model input*

A distillation column was modeled applying an equilibrium stage model which is based on the MESH (Material, Equilibrium, Summation and Heat balance) (Seader et al., 2008). The RadFrac model available in the Aspen Plus V11 was adopted to simulate the distillation column. Further, the NRTL-RK thermodynamic model was employed in the modeling, and the binary parameters were taken from databank (APV110 VLE–RK) for every component pair in Table 2. The binary interaction parameters for styrene + αMS and toluene + styrene was adopted from the previous work (Dahal et al., 2023).

Firstly, a reasonable number of stages were selected, and some preliminary tests with a side draw and a feed location was made. The selected column configuration allows sufficient separation between the lighter components and the styrene side draw at the top of the column, the separation of styrene product from the dimers and the heavier components between the side draw and the feed, and the recovery of styrene from the heavy bottom product below the feed point. The stages are numbered top to bottom in the simulation.

After the preliminary tests, a distillation column was configured. The distillation column was assumed to consist of 50 equilibrium stages with three outgoing streams: a distillate, a bottom and a side stream as shown in Fig. 3. The condenser pressure was set to 50 mbar to keep the column temperature lower and minimize the risk of styrene polymerization. A similar pressure was applied in the distillation column design for the separation of styrene and ethylbenzene by Jongmans and co-authors (Jongmans et al., 2012). The saturated liquid feed was fed to the distillation column with the feed composition provided in Table 2. The PS pyrolysis oil was fed at the stage 35 and pure styrene side stream was located at the stage 10. The purity of styrene in the side

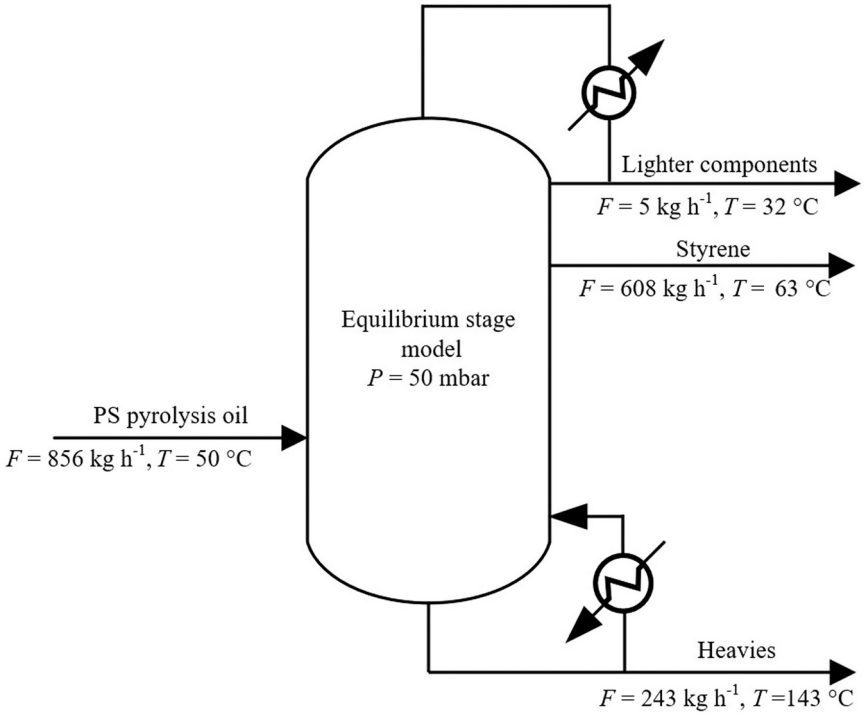

Fig. 3 – Process scheme of the distillation column with the flowrates along with the temperatures of the streams for the separation of pure styrene monomer from the polystyrene pyrolysis oil.

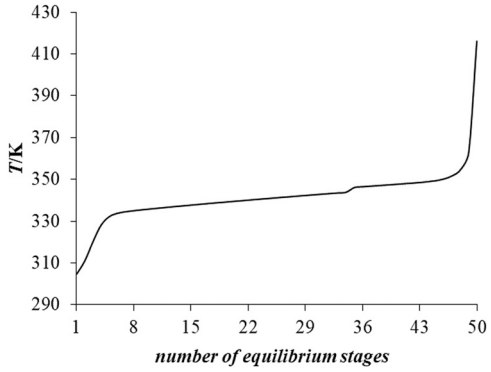

Fig. 4 – Temperature profile from simulation as a function of equilibrium stages.

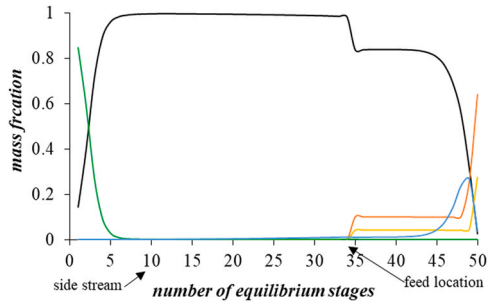

Fig. 5 – Liquid composition profile from simulation as a function of equilibrium stages for (—) toluene, (—) styrene, (—) dimer, (—) heavier fraction or trimer and (—) α-methylstyrene.

stream was set to 0.996 and the recovery of styrene in the bottoms was kept 0.01 in mass fraction. The liquid side stream and the reflux rates were allowed to vary as adjustable variables between the upper and the lower bounds in the column specifications during the simulation.

5.2. *Simulation results*

From the process scheme in Fig. 3, the lighter and the heavier components than styrene were obtained from the distillate and the bottom streams, respectively. Similarly, the pure styrene was recovered from the side stream. The temperature profile and the composition profile of a few selected key components of the PS pyrolysis oil is displayed in Figs. 4 and 5, respectively. Fig. 4 shows that the bottoms temperature increases steeply as the low boiling fractions and styrene are distilled, and the high boiling fraction increases in the bottoms.

Fig. 5 illustrates that toluene is one of the key components obtained from the distillate. This distillate could be further purified to aromatic streams; however, a feasibility study needs to be carried out before the separation as the distillate is a small stream of close boiling components. Fig. 5 also shows a sharp separation between the styrene and its oligomers. Due to this reason, styrene can be acquired with a high purity.

The bottoms fraction consists of styrene oligomers in Fig. 5; therefore, the bottoms stream could be recycled back to the pyrolysis unit to increase the styrene content in the PS pyr-

olysis oil. However, the separation of the lighter aromatics than oligomers (Table 2) is required before recycling the bottoms stream into the pyrolysis unit due to obvious reasons. Firstly, even after further pyrolysis these lighter aromatics do not contribute to increase the styrene content in the pyrolysis oil. Secondly, as the lighter fractions increases there are chances of having these lighter fractions in the pure styrene stream which will affect the purity of styrene. Further, αMS seems to be a potential component from the heavier fraction to affect the purity of styrene during the separation as implied in Fig. 5. This was also observed from the short-path distillation results in Section 4.2.

Therefore, it would be suitable from the process optimization viewpoint to leave a small fraction of styrene in the bottom due to various reasons as follows:

i. This helps to keep the temperature of the bottoms lower and minimize the risk of polymerization.
ii. The presence of styrene in the bottoms lowers the density of the bottoms and makes it easily pumpable as the dimer and the trimer range components have higher densities and are solid at room temperature.
iii. It would decrease the probability of having αMS or any other aromatics lighter than oligomers as an impurity in the pure styrene stream.

6. Discussion

6.1. *Polystyrene pyrolysis products*

The GC analysis from this work shows that the pyrolysis of PS yields dominating components: styrene, dimer, and trimer in Table 2. A similar analysis was provided in the literature (Scott et al., 1990; Onwudili et al., 2009; Scheirs and Kaminsky, 2006). Besides styrene monomer and oligomers, other aromatics have also been identified as the PS pyrolysis oil components in this work in Table 2 as well as in the literature (Liu et al., 2000; Onwudili et al., 2009). This shows that the components present in the PS pyrolysis oil (Table 2) can be divided into four categories which are i) the aromatics lighter than styrene, ii) styrene, iii) the aromatics lighter than styrene oligomers and iv) the styrene oligomers.

Based on these product types, the degradation scheme of polystyrene can be proposed such that the larger molecules degrade to styrene and its oligomers. The other aromatics are the reaction products formed during the pyrolysis. However, in this work the reaction scheme of polystyrene during the pyrolysis was not a part of the study. The proposed degradation scheme of polystyrene is a preliminary idea based on the products analyzed in the PS pyrolysis oil.

The proposed degradation scheme of polystyrene was compared with the reaction schemes presented in the literature to acquire a better understanding. A similar reaction scheme have been studied in the earlier publications where the main type of reaction is the cleavage of larger molecules to its monomeric units (Hua et al., 2022) and the reaction of styrene itself to various end products (Onwudili et al., 2009; Hua et al., 2022).

7. Conclusions

This work presents the distillation column characterization and the experimental batch distillation for the purification of pure styrene monomer from the polystyrene pyrolysis oil. The distillation column was firstly characterized with the known systems to obtain information about the number of theoretical stages, the height equivalent theoretical plate, the heat losses, the pressure drop and the column hold-up. Thereafter, the distillation of the polystyrene pyrolysis oil was performed in a batch mode, and five distillate fractions were obtained. From the GC analysis, the mass fraction of styrene in the distillate fraction was 0.9994. However, it was necessary to stop distillation at bottoms temperature of 100–120 °C due to the risk of polymerization. The bottoms fraction from the batch distillation was further fractionated using a short-path distillation unit to study the separation of most of the styrene from the polystyrene pyrolysis oil. Additionally, the viscosities and the densities of the bottom fractions were measured at the temperature range of 298–348 K.

A batch distillation was modeled applying the experimental conditions. The model predictions agree well with the experimental temperature and time profile. Furthermore, a process scheme was proposed to enable a continuous distillation for real size unit. The simulation model suggests that it is possible to obtain a high-purity stream from the pyrolyzed polystyrene plastics by using a single-distillation column with a side-draw for the main styrene product.

Declaration of Competing Interest

The authors declare that they have no known competing financial interests or personal relationships that could have appeared to influence the work reported in this paper.

Acknowledgements

Roshi Dahal acknowledges the financial support of Fortum and Neste Foundation for post-graduate studies. Business Finland is acknowledged for the funding of MoPo Multitechnological recycling of polystyrene 1545/31/2020 - project. Academy of Finland is acknowledged for the funding of FIRI2016 project. Aleksi Vartiainen is greatly acknowledged for performing distillation runs, analysis of distillate fractions and reporting. Many thanks to Dr. Juha Linnekoski for the GCMS laboratory support. I am grateful to Maurice Forget for reading and providing suggestions for the language improvement.

Appendix

see Table A1.

Table A1 – Settings for Agilent 6850 gas chromatograph.

GC name	Agilent 6850	
	Column	
Type	Capillary	
Model number	Agilent 19091 N-216E	
Column coating material	HP-INNOWax Polyethylene Glycol	
Nominal length/m	60	
Nominal diameter/μm	320	
Nominal film thickness/μm	0.5	
	Detector	
Type	FID	
Temperature/K	573.15	
Method	I	II
Inlet		
Mode	Split	Split
Temperature/K	548.15	523.15
Pressure/kPa	92.0	52.0
Split ratio	50:1	100:1
Gas type	He	He
Total flow/mL.min^{-1}	84.5	68.8
Split flow/mL.min^{-1}	80.4	65.7
Oven		
Initial/K	313.15	348.15
Hold time/min	1	23
-Ramp:		
Ramp rate/C.min^{-1} to Final temperature/K	30–523.15	ramp 1.3–373.15, then ramp 4.4–493.15
Run time/min	33	1st ramp: 42.23, 2nd ramp: 69.50
Post run		
T/K	523.15	493.15
Run time/min	5	5

Appendix A. Supporting information

Supplementary data associated with this article can be found in the online version at doi:10.1016/j.cherd.2023.05.039.

References

Barnes, D.K.A., Galgani, F., Thompson, R.C., Barlaz, M., 2009. Accumulation and fragmentation of plastic debris in global environments. Philos. Trans. R. Soc. B 364, 1985–1998.

Jambeck, J.R., Geyer, R., Wilcox, C., Siegler, T.R., Perryman, M., Andrady, A., Narayan, R., Law, K.L., 2015. Plastic waste inputs from land into the ocean. Science 347, 768–771.

Qureshi, M.S., Oasmaa, A., Pihkola, H., Deviatkin, A., Tenhunen, A., Mannila, J., Minkkinen, H., Pohjakallio, M., Laine-Ylijoki, J., 2020. Pyrolysis of plastic waste: Opportunities and challenges. J. Anal. Appl. Pyrolysis 152, 104804.

Rahimi, A.R., Garciá, J.M., 2017. Chemical recycling of waste plastics for new materials production, Nature Reviews. Chemistry 1, 46.

Hopewell, J., Dvorak, R., Kosior, E., 2009. Plastics recycling: challenges and opportunities. Philos. Trans. R. Soc. B: Biol. Sci. 364, 2115–2126.

Ellen MacArthur Foundation, The New Plastics Economy: Rethinking the Future of Plastics & Catalysing Actions (2017).

Grause, G., Buekens, A., Sakata, Y., Okuwaki, A., Yoshioka, T., 2011. Feedstock recycling of waste polymeric material. J. Mater. Cycles Waste Manag 13, 265–282.

Sharma, B.K., Moser, B.R., Vermillion, K.E., Doll, K.M., Rajagopalan, N., 2014. Production, characterization, and fuel properties of alternative diesel fuel from pyrolysis of waste plastic grocery bags. Fuel Process. Technol. 177, 79–90.

Liu, Y., Qian, J., Wang, J., 2000. Pyrolysis of polystyrene waste in a fluidized-bed reactor to obtain styrene monomer and gasoline fraction. Fuel Process. Technol. 63, 45–55.

Dahal, R., Uusi-Kyyny, P., Pokki, J.-P., Alopaeus, V., 2023. Isobaric vapor–liquid equilibrium of the binary mixtures toluene + styrene and styrene + α–methylstyrene. J. of Chem. Eng. Data 68 (3), 654–663.

Kim, T.H., Lee, K., Oh, B.R., Lee, M.E., Seo, M., Li, S., Kim, J.K., Choi, M., Chang, Y.K., 2021. A novel process for the production biojet fuel and high-value polyunsaturated fatty acid esters from heterotrophic microalagae Schizochytrium sp. ABC101. Renew. Enery 165, 481–490.

Seader, J.D., Henley, E.J., Roper, D.K., 2008. Separation Process Principles Chemical and Biochemical Operations, Third Edition. John Wiley & Sons, Inc. United States of America.

Design Institute for Physical Properties, Sponsered by AIChE (2005; 2008; 2009; 2010; 2011; 2012; 2015; 2016; 2017; 2018; 2019; 2020; 2021) DIPPR Project 801 - Full Version.

Tsuge, S., Ohtani, H., Watanabe, C. Pyrolysis-GC/MS data book of Synthetic Polymers: Pyrograms, Thermograms and MS of

Pyrolyzates, First Edition, 2011 ©Elsevier B.V. Printed by CPI Group Ltd, Croydon, United Kingdom.
Baird, Z.S., Uusi-Kyyny, P., Oja, V., Alopaeus, V., 2017. Hydrogen solubility of shale oil containing polar phenolic compounds. Ind. Chem. Eng. Res. 56, 8738–8747.
Dahal, R., Uusi-Kyyny, P., Pokki, J.P., Alopaeus, V., 2021. Vapor-liquid equilibrium for the n-dodecane + phenol and n-hexadecane + phenol systems at 523 K and 573 K. Fluid Phase Equilibria 537, 112991.
Renon, H., Prausnitz, J.M., 1968. Local compositions in thermodynamic excess functions for liquid mixtures. AIChE J. 14, 135–144.
Redlich, O., Kwong, J.N.S., 1949. On the thermodynamics of solutions. V. An equation of state. Fugacities of gaseous solutions. Chem. Rev. 44, 233–244.
Jongmans, M.T.G., Hermens, E., Raijmakers, M., Maassen, J.I.W., Schuur, B., de Haan, A.B., 2012. Conceptual process design of extractive distillation processes for ethylbenzene/styrene separation. Chem. Eng. Res. Des. 90, 2086–2100.
Scott, D.S., Czernik, S.R., Piskorz, J., Radlein, D.St.A.G., 1990. Fast pyrolysis of plastic waste. Energy Fuels 4, 407–411.
Onwudili, J.A., Insura, N., Williams, P.T., 2009. Composition of products from the pyrolysis of polyethylene and polystyrene in a closed batch reactor: effects of temperature and residence time. J. Anal. Appl. Pyrolysis 86, 293–303.
Scheirs, J., Kaminsky, W., 2006. Feedstock Recycling and Pyrolysis of Waste Plastics–Converting Waste Plastics into Diesel and other Fuels. In: Wiley Series in Polymer Science. John Wiley & Sons Ltd, United Kingdom.
Hua, F., Fu, Z., Cheng, Y., 2022. A simplified and effective molecular-level kinetic model for plastic pyrolysis. Chem. Eng. Sci. 264, 118146.